

## Removal of Atmospheric Pollutants

### (6) Absorption of Lean NO in Aqueous Slurries of Ca(OH)<sub>2</sub> with NaClO<sub>2</sub> or Mg(OH)<sub>2</sub> with NaClO<sub>2</sub>

Ichibei KUDO, Takashi KONDO, Eizo SADA\*,  
and Hidehiro KUMAZAWA\*

### 大気汚染物質除去に関する研究

#### (6) Ca(OH)<sub>2</sub>, NaCl<sub>2</sub>とMg(OH)<sub>2</sub>, NaClO<sub>2</sub> スラリーによる希薄NOの吸収

工藤市兵衛・近藤高司・佐田栄三\*・熊沢英博\*

The absorption of lean NO in an aqueous slurry of Ca(OH)<sub>2</sub> or Mg(OH)<sub>2</sub> with NaClO<sub>2</sub> was carried out using a stirred tank absorber with a plane gas-liquid interface at 25°C and 1 atm. The rates of absorption of NO and the accompanying desorption of NO<sub>2</sub> for the Ca(OH)<sub>2</sub> slurry were in close agreement with those for the aqueous mixed solution of NaClO<sub>2</sub> and NaOH with higher OH<sup>-</sup> concentration, whereas for the Mg(OH)<sub>2</sub> slurry, the absorption rate of NO noticeably exceeded that for the former systems. Furthermore, the ratio of the NO<sub>2</sub> desorption rate to the NO absorption rate considerably exceeded the theoretical prediction for gas absorption with the consecutive reaction (maximum deviation attained 117 %). Also, chlorine dioxide was detected in the gas phase. It was deduced from these experimental evidences that there occur both desorption of the decomposition product ClO<sub>2</sub> and gas-phase oxidation of NO with ClO<sub>2</sub> to produce NO<sub>2</sub>.

## INTRODUCTION

In the previous work [1,2], the absorption of lean NO in aqueous mixed solutions of NaClO<sub>2</sub> and NaOH was carried out using a stirred vessel with a plane gas-liquid interface, and the chemical absorption kinetics was analyzed. As a result, the following information was derived. In the high NO concentration region greater than 2000 ppm, the order of reaction with respect to NO was estimated as 2, whereas for the NO concentration less than several hundred ppm, the reaction order varied from 2 to 1 with decreasing the NO concentration. The order of reaction of NaClO<sub>2</sub> was determined as unity only for the NaClO<sub>2</sub> concentration greater than 0.8 molar. For the concentration less than 0.8 molar, the dependence on the concentration becomes markedly and a simple relationship was not extracted. When the concentration of NaClO<sub>2</sub> exceeds 0.8 molar and the partial pressure of NO exceeds 0.002 atm, the reaction between NO and NaClO<sub>2</sub> in an aqueous solution can be regarded as second-order in NO and first-order in

NaClO<sub>2</sub>. The effect of the NaOH concentration on the third-order rate constant  $k$  was expressed by  $k = 3.80 \times 10^{12} \exp(-3.73 [\text{NaOH}])$  in the range of  $0.5 < [\text{NaOH}] < 0.5$  molar. In considering this result, the rate of the reaction increases with decreasing the NaOH concentration, but too low concentration of OH<sup>-</sup> results in decomposition of NaClO<sub>2</sub>. Then a decomposition product ClO<sub>2</sub> is evolved in the gas phase and the gas-phase oxidation of NO takes place. Hence in order to suppress the decomposition of NaClO<sub>2</sub> and give the absorbent a stable oxidation ability, it is necessary to keep the OH<sup>-</sup> concentration to a value. However, if a depletion of OH<sup>-</sup> due to the reaction can be prevented, then the decomposition of NaClO<sub>2</sub> may be suppressed even when the concentration of OH<sup>-</sup> is kept low. Such a situation is established by using sparingly soluble alkaline-earth hydroxide as an alkali source. An aqueous slurry of Ca(OH)<sub>2</sub> or Mg(OH)<sub>2</sub> has low concentration of OH<sup>-</sup> but high alkaline capacity. Thus, in the present work, the absorption rate of NO by an aqueous slurry of Ca(OH)<sub>2</sub> with NaClO<sub>2</sub> or Mg(OH)<sub>2</sub> with NaClO<sub>2</sub> in a

This paper has been published in Chem. Eng. Sci., 719,34 (1979).

\* 京都大学工学部

stirred vessel was measured and the absorption mechanism was analyzed in terms of the chemical absorption theory.

## EXPERIMENTAL

All the absorption runs were made using a stirred tank absorber with a plane gas-liquid interface at 25 °C and 1 atm. The absorber used (I.D.=80 mm, Liquid volume=500 cm<sup>3</sup>) is the same as in the previous work [1,2]. The absorber was operated continuously with respect to the gas phase and batchwise with respect to the liquid phase. Two stirrers driven by two separate motors were used to agitate the gas and liquid phases. The stirring speeds of the liquid phase and gas phase stirrers were maintained at 162 and 500 rpm, respectively. The concentration of NO in the feed stream was varied from 50 to 800 ppm. The concentrations of NO and NO<sub>2</sub> in the gas phase were determined by UV derivative spectrophotometer (Yanaco UO-1). Absorption rates of NO were calculated from the difference between inlet and outlet concentrations of NO and the total gas flow rate. Also, desorption rate of NO<sub>2</sub> were calculated from the outlet concentration of NO<sub>2</sub> and the total gas flow rate.

## EXPERIMENTAL RESULTS AND DISCUSSION

### 1. Absorption of NO in an aqueous slurry of Ca(OH)<sub>2</sub> with NaClO<sub>2</sub>

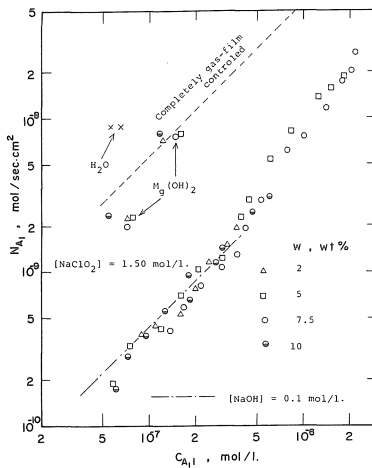


Fig. 1. Absorption rates of NO for the NaClO<sub>2</sub>/Ca(OH)<sub>2</sub> slurry system.

Figure 1 shows absorption rates of NO in aqueous slurries of Ca(OH)<sub>2</sub> with NaClO<sub>2</sub> under various NO concentrations. The liquid phase contains 2, 5, 7.5 and 10 wt% of fine Ca(OH)<sub>2</sub> particles in an aqueous NaClO<sub>2</sub> solution. The OH<sup>-</sup> concentration in the aqueous solution saturated with Ca(OH)<sub>2</sub> amounts to

0.046 g-ion/l. It is apparent that experimental absorption rates are not influenced by the solid concentration. The dot-dash line represents the absorption rate of NO by an aqueous mixed solution of 1.5 molar NaClO<sub>2</sub> and 0.1 molar NaOH [2]. In the range of C<sub>A11</sub> < 5 × 10<sup>-7</sup> mol/l, the slope of the dot-dash line approximately equals unity, which implies that the reaction between NO and NaClO<sub>2</sub> in an alkaline solution can be expressed by first-order with respect to NO. When using Ca(OH)<sub>2</sub> as an alkaline source, the OH<sup>-</sup> concentration in a slurry (0.046 g-ion/l) corresponds to about half the value for the dot-dash line. These, the reaction rate constant for the slurry solution is increased by c.a. 22 percent, but the absorption rate increases only by c.a. 11 percent. In this way, experimental absorption rates fall closely on the dot-dash line within the experimental error. The experimental result that the absorption rate is not influenced by the slurry concentration may be expected from the theoretical prediction that the absorption process lies under the fast-reaction regime.

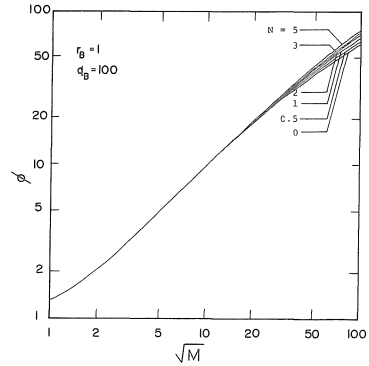


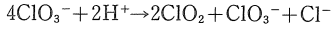
Fig. 2. Dependence of the parameter N on the enhancement factor for the slurry system.

Figure 2 indicates the relationship between enhancement factor and reaction-diffusion modulus as a parameter of N for gas absorption with a second-order reaction in slurry (A(g) → AB(aq), B(s) → (aq), A(aq) + νB(aq) → products). The parameter N is defined by  $k_s A_p z^2 L / D_B$ , where  $A_p$  is equal to  $6w / \rho d_p$ , and hence is proportional to solid concentration w. This figure clearly shows that the relation of  $\Phi$  vs  $\sqrt{M}$  is almost independent of N or w in a fast-reaction regime. The rates of NO absorption in a slurry of Ca(OH)<sub>2</sub> with NaClO<sub>2</sub> may be expected from the previous work [2], and it is deduced that NaClO<sub>2</sub> in absorbent is not excessively decomposed.

### 2. Absorption of NO in an aqueous slurry of Mg(OH)<sub>2</sub> with NaClO<sub>2</sub>

In an aqueous solution saturated with Mg(OH)<sub>2</sub>, the OH<sup>-</sup> concentration is equal to 0.00092 g-ion/l.

As the absorption of NO proceeds, the pH of the absorbent near the gas-liquid interface may shift above 7, because reaction products through reaction (iii) described later,  $\text{HNO}_3$  and  $\text{HNO}_2$ , are accumulated. In an acidic solution, the absorbent  $\text{NaClO}_2$  decomposes to form  $\text{ClO}_2$ :



The absorption spectra of the chlorine dioxide evolved from an aqueous solution of  $\text{NaClO}_2$  with 1.

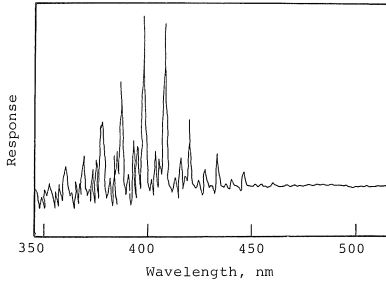


Fig. 3. Absorption spectra of  $\text{ClO}_2$  evolved from aqueous  $\text{NaClO}_2$  solution by adding  $\text{H}_2\text{SO}_4$ .

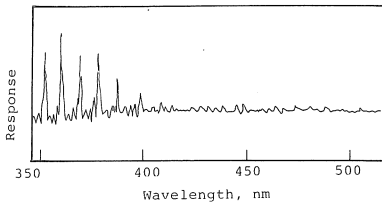


Fig. 4. Absorption spectra of effluent gas.

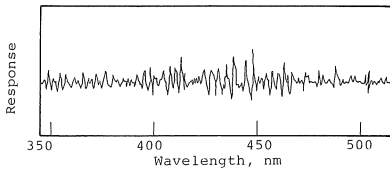


Fig. 5. Absorption spectra of  $\text{NO}_2$  diluted with  $\text{N}_2$ .

5 molar by adding small amount of  $\text{H}_2\text{SO}_4$  are shown in Fig. 3. The absorption spectra here are the second-order derivative of the direct (conventional) absorption spectra. A series of characteristic peaks identifying  $\text{ClO}_2$  appears in the range of wave length of 350 nm-450nm. Figure 4 indicates the measurements of absorption spectra of the effluent gas during the NO absorption, whereas Figure 5 shows the absorption spectra of  $\text{NO}_2$  only diluted with  $\text{N}_2$ . Judging from comparison of absorption spectra depicted in Figs. 3 through 5, there exists  $\text{ClO}_2$  in the effluent gas during the NO absorption. That is, the form of absorption spectra in the range of 350-400nm in wave length in Fig. 4

suggests the presence of  $\text{ClO}_2$ . On the other hand, it is considered that the absorption spectra for chlorine overlap on those for nitrogen dioxide, but chlorine could not be detected because the molecular extinction coefficient for chlorine is much lower than that for nitrogen dioxide. (Thus, in the analyzer used, the lowest limit of detection for chlorine was about 5000 ppm.)

Figure 6 shows a typical example of variation of the absorption rate ( $N_{A1}$ ) and the degree of removal of NO with the process time. The time required to reach the steady-state in the absorption process, is increasing with an increase in solid concentration, but the absorption rate at steady-state is independent of the solid concentration. The steady-state absorption rate, which is plotted against the interfacial concentration in Fig. 1, is enough high not to be expected from the results for the aqueous slurry of  $\text{Ca}(\text{OH})_2$  with  $\text{NaClO}_2$  as well as the aqueous mixed solution of  $\text{NaClO}_2$  and  $\text{NaOH}$ . It is reduced from detected components in the effluent gas that such high absorption rates are attributed to the existence of the gas-phase oxidation of NO with  $\text{ClO}_2$ . In Fig. 6 is also shown the variation of the

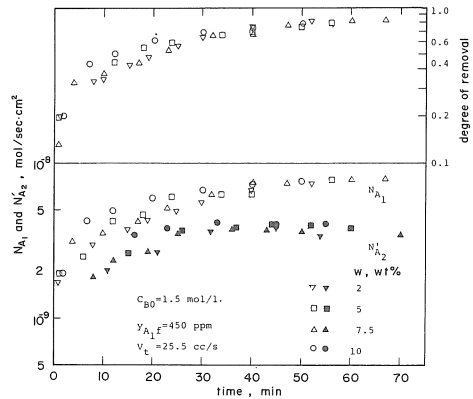


Fig. 6. Absorption rate of NO and desorption rate of  $\text{NO}_2$  for the  $\text{NaClO}_2/\text{Mg}(\text{OH})_2$  slurry system. Effect of solid concentration.

desorption rate of  $\text{NO}_2$  (including the production rate of  $\text{NO}_2$  due to the gas-phase oxidation of NO with  $\text{ClO}_2$ ) with the process time. From the figure, the ratio  $N'_{A2}/N_{A1}$  at steady-state attains 0.43~0.52. Also, for  $y_{A1F} = 215$  ppm,  $N'_{A2}/N_{A1}$  attained 0.28~0.41. For the  $\text{NaClO}_2/\text{Ca}(\text{OH})_2$  slurry system, on the other hand, the ratio for  $y_{A1F} = 205$  ppm reduced to 0.16~0.19. This magnitude can be predicted from the simulation of gas absorption with the consecutive reaction whose mechanism and kinetics are well defined in the previous work [1,2]

Figure 7 shows the effect of  $\text{NaClO}_2$  concentration on the rate of NO absorption  $N_{A1}$  and the rate of  $\text{NO}_2$  desorption (including gas-phase production)  $N'_{A2}$ . The  $\text{NaClO}_2$  concentration has negligible effect

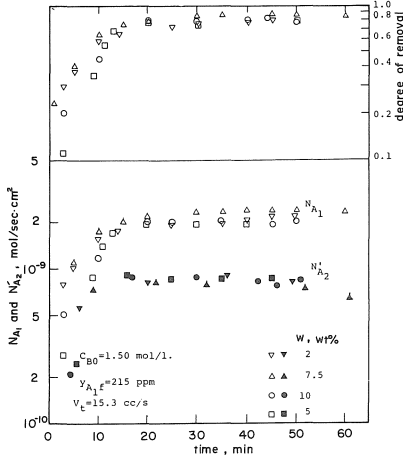
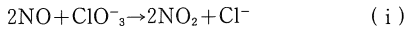


Fig. 7. Absorption rate of NO and desorption rate of NO<sub>2</sub>. Effect of NaClO<sub>2</sub> concentration.

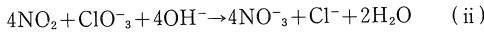
on the variation of  $N_{A1}$  and  $N'_{A2}$  with time. This fact favorably supports the speculation that there considerably exists a conversion of NO to NO<sub>2</sub> in the gas phase.

### 3. Simulation of the processes of the NO absorption and the accompanying NO<sub>2</sub> desorption

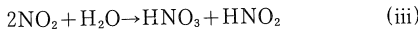
Dissolved NO reacts with ClO<sub>2</sub><sup>-</sup> in an alkaline solution of NaClO<sub>2</sub> to produce NO<sub>2</sub> by



Some of NO<sub>2</sub> produced is consumed by the liquid-phase reactions:

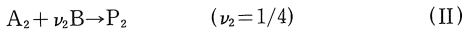
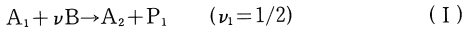


and



Some evolves into the gas phase without undergoing any chemical reaction. In the following, the processes of the NO absorption and the accompanying NO<sub>2</sub> desorption are formulated on the basis of the film model, and the magnitude of the ratio of NO<sub>2</sub> desorption rate to NO absorption rate will be estimated.

The reactions relevant to NO and NO<sub>2</sub> can be described by the following relations:



First, the problem will be considered for the absorption of NO in an aqueous mixed solution of 1.5 molar NaClO<sub>2</sub> and 0.2 molar NaOH. The gas-phase concentration of NO is put 1250 ppm ( $C_{A11} = 2 \times 10^{-6}$  mol/l), where the reaction rate expression is well established [1]. Under such a high concentration region, reaction (I) can be expressed by second-order

in NO (A<sub>1</sub>) and first-order in NaClO<sub>2</sub> (B) and its rate constant at 25 °C is estimated as  $1.8 \times 10^{12}$  (1/mol)<sup>2</sup>/sec [1]. Reaction (II) is found to be second-order in NO<sub>2</sub> (A<sub>2</sub>) and first-order in NaClO<sub>2</sub> (B) and the third-order reaction rate constant at 25 °C is derived to be  $7.32 \times 10^8$  (1/mol)<sup>3</sup>/sec [2]. Reaction (III) (hydrolysis of NO<sub>2</sub>) can be also expressed by second-order in NO<sub>2</sub> and its rate constant at 25 °C is derived as  $3.09 \times 10^8$  1/mol sec [2].

When Reactions (I), (II) and (III) are taking place in the liquid phase, mass balance equations for components A<sub>1</sub>, A<sub>2</sub> and B can be written as follows:

$$D_{A1} \frac{d^2 C_{A1}}{dz^2} = k_1 C_{A1}^2 C_B \quad (1)$$

$$D_{A2} \frac{d^2 C_{A2}}{dz^2} = k_{II} C_{A2}^2 C_B + k_{hyd} C_{A2}^2 - k_I C_{A1}^2 C_B \quad (2)$$

$$D_B \frac{d^2 C_B}{dz^2} = \nu_1 k_I C_{A1}^2 C_B + \nu_2 k_{II} C_{A2}^2 C_B \quad (3)$$

The boundary conditions are given by

$$\left. \begin{aligned} \text{at } z = 0; \quad C_{A1} &= C_{A1i}, \\ D_{A2} \frac{dC_{A2}}{dz} &= k_{GA2} (C_{A2i} - C_{A2g}), \\ \frac{dC_B}{dz} &= 0 \end{aligned} \right\} \quad (4)$$

$$\text{at } z = z_L; \quad C_{A1} = C_{A2} = 0, \quad C_B = C_{B0} \quad (5)$$

The mass balance equations and boundary conditions may be put into the following dimensionless form:

$$\frac{d^2 Y_{A1}}{dx^2} = M_1 Y_{A1}^2 Y_B \quad (6)$$

$$\frac{d^2 Y_{A2}}{dx^2} = \left( \frac{M_1 s r_2}{r_1} \right) Y_{A2}^2 Y_B + \left( \frac{M_1 s' r_2}{r_1} \right) Y_{A2}^2 - \left( \frac{M_1 r_2}{r_1} \right) Y_{A1}^2 Y_B \quad (7)$$

$$\frac{d^2 Y_B}{dx^2} = \left( \frac{M_1}{r_1 q_1} \right) Y_{A1}^2 Y_B + \left( \frac{M_1 s}{r_1 q_2} \right) Y_{A2}^2 Y_B \quad (8)$$

$$\left. \begin{aligned} \text{at } x = 0; \quad Y_{A1} &= 1, \\ \frac{dY_{A2}}{dx} &= B_1 (Y_{A2i} - Y_{A2g}), \\ \frac{dY_B}{dx} &= 0 \end{aligned} \right\} \quad (9)$$

$$\text{at } x = 1; \quad Y_{A1} = Y_{A2} = 0, \quad Y_B = 1 \quad (10)$$

The parameters included in Eqs. (6) to (10) take following quantities for the conditions developed here:

$$s = \frac{k_{II}}{k_I} = 4.07 \times 10^{-4} \quad s' = \frac{k_{hyd}}{k_I C_{B0}} = 1.14 \times 10^{-4}$$

$$q_1 = \frac{C_{BO}}{\nu_1 C_{A1i}} = 1.5 \times 10^5 \quad q_2 = \frac{C_{BO}}{\nu_2 C_{A1i}} = 3 \times 10^6$$

$$M_1 = 3.12 \times 10^7 \quad r_1 = 0.745 \quad r_2 = 1.35$$

The Biot number  $B_1$  takes 730 under the present experimental conditions and  $Y_{A2g}$  is assumed to be zero.

The above ordinary differential equations, Eqs. (6) to (8), are nonlinear; therefore analytical solutions are not expected. Then, a set of differential equations were approximated by the time-centered implicit finite difference equations. These implicit equations were simplified by linearizing the reaction terms. A set of resultant simultaneous linear equations was solved by the method of tridiagonal equations. Numerical results were expressed in terms of enhancement factor  $\phi_{A1}$  and ratio  $N'_{A2}/N_{A1}$  defined by

$$\phi_{A1} = - \left( \frac{dY_{A1}}{dx} \right)_{x=0} \quad (11)$$

and

$$\frac{N'_{A2}}{N_{A1}} = \left( \frac{r_1}{r_2 \phi_{A1}} \right) \left( \frac{dY_{A2}}{dx} \right)_{x=0} \quad (12)$$

as a function of reaction-diffusion modulus  $\sqrt{M_1}$

In the course of computation, scales of  $q_1$  and  $q_2$  were reduced by  $10^3$  because of rapid convergence. Thereby  $M_1$  decreases by a factor  $10^{-3}$ , whereas  $s'$  increases by a factor  $10^3$ . Numerical results are shown in fig. 8.  $N'_{A2}/N_{A1}$  is calculated as 0.29 when

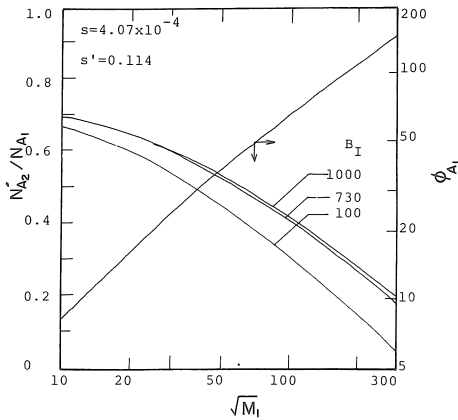


Fig. 8. Theoretical relation of  $N'_{A2}/N_{A1}$  vs  $\sqrt{M_1}$  and  $\phi_{A1}$  vs  $\sqrt{M_1}$  for the NO- $\text{NaClO}_2/\text{NaOH}$  system.

$\sqrt{M_1} = 177$  and  $B_1 = 730$ .

For the  $\text{NaClO}_2/\text{Ca}(\text{OH})_2$  slurry system,  $\text{OH}^-$  concentration is evaluated 0.046 g-ion/l; thereby  $k_1 = 3.20 \times 10^{12}$  (1/mol)<sup>2</sup>/sec and  $s' = 0.0644$ . The  $s$  value is assumed to be equal to that for the previous case ( $s = 4.07 \times 10^{-4}$ ). In this case,  $q_1$  and  $q_2$  are also reduced by a factor  $10^3$ . Figure 9 shows computational result as a plot of  $N'_{A2}/N_{A1}$  vs  $\sqrt{M_1}$ , where  $N'_{A2}/N_{A1}$  is obtained

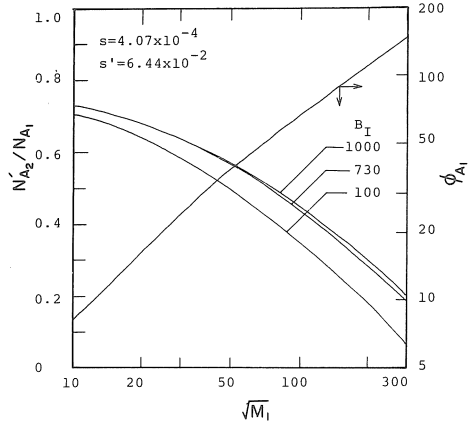


Fig. 9. Theoretical relation of  $N'_{A2}/N_{A1}$  vs  $\sqrt{M_1}$  and  $\phi_{A1}$  vs  $\sqrt{M_1}$  for the NO- $\text{NaClO}_2/\text{Ca}(\text{OH})_2$  system.

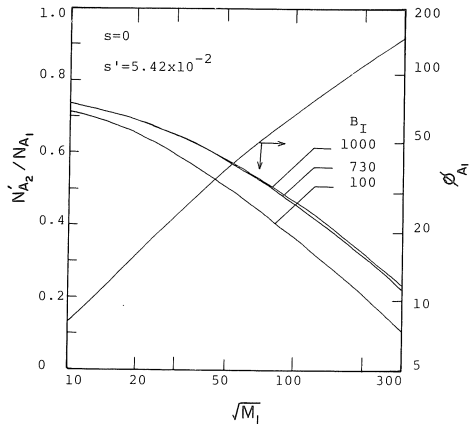


Fig. 10. Theoretical relation of  $N'_{A2}/N_{A1}$  vs  $\sqrt{M_1}$  and  $\phi_{A1}$  vs  $\sqrt{M_1}$  for the NO- $\text{NaClO}_2/\text{Mg}(\text{OH})_2$  system.

as 0.24 when  $\sqrt{M_1} = 235$ , and  $B_1 = 730$ . This prediction a bit exceeds experimental results (0.16 to 0.19).

For the  $\text{NaClO}_2/\text{Mg}(\text{OH})_2$  system, the  $\text{OH}^-$  concentration is negligibly small and there appears no contribution is negligibly small and there appears no contribution of reaction (II). Therefore  $s = 0$ . The  $s'$  value reduces to 0.0542 ( $k_1 = 3.80 \times 10^{12}$  (1/mol)<sup>2</sup>/sec). Numerical results are shown in Fig. 10.  $N'_{A2}/N_{A1}$  is calculated as 0.24 when  $\sqrt{M_1} = 284$  and  $B_1 = 730$ . On the other hand, experimental values of  $N'_{A2}/N_{A1}$  ranged from 0.43 to 0.52 for  $y_{A1f} = 450$  ppm as shown in Fig. 6 and from 0.28 to 0.41 for  $y_{A1f} = 215$  ppm. It also suggests that there significantly occur both desorption of the decomposition product  $\text{ClO}_2$  into the gas phase and gas-phase oxidation of NO with  $\text{ClO}_2$  to produce  $\text{NO}_2$ .

## CONCLUSION

The rates of absorption of NO and the accompanying desorption of NO<sub>2</sub> the NaClO<sub>2</sub>/Ca(OH)<sub>2</sub> slurry system, were satisfactorily expected from the previous observation in the aqueous mixed solution of NaClO<sub>2</sub> and NaOH with higher OH<sup>-</sup> concentration, whereas for the NaClO<sub>2</sub>/Mg(OH)<sub>2</sub> slurry system, the absorption rate of NO noticeably exceeded that for the former systems and the ratio of the NO<sub>2</sub> desorption rate to the NO absorption rate considerably exceeded the theoretical prediction for gas absorption with the consecutive reaction. The maximum deviation between two factors has attained 117 %. Also, chlorine dioxide was detected in the gas phase. It was deduced from these experimental evidences that there significantly occur both desorption of the decomposition product ClO<sub>2</sub> into the gas phase and gas-phase oxidation of NO with ClO<sub>2</sub> to produce NO<sub>2</sub>.

Acknowledgements—The authors wish to express their thanks to Japan Securities Scholarship Foundation for its financial support.

## NOTATION

$A_p$	surface area of solid particles = $6w/pd_p$ , cm <sup>2</sup> /cm <sup>3</sup> -dispersion
$B_i$	Biot number = $k_{GA2}/k_{LA2}$
$C$	concentration in liquid phase, mol/cm <sup>3</sup> or mol/l

$D$	diffusivity in liquid phase, cm <sup>2</sup> /sec
$d_p$	average diameter of solid particles, cm
$k_{II}$	rate constant of reaction (II), (l/mol <sup>2</sup> )/sec
$k_L$	mass transfer coefficient in liquid phase, cm/sec
$M_1$	reaction-diffusion modulus = $k_i C_{A11} C_{B0} / (k_{LA1})^2$
$V_t$	total gas flow rate, cm <sup>3</sup> /sec
$W$	concentration of solid, g/cm <sup>3</sup> -dispersion of wt%
*	relative to that in the bulk of liquid or at solid surface
$\rho$	density of solid, g/cm <sup>3</sup>
○	without chemical reaction

## REFERENCES

- [1] Sada E., Kumazawa H., Kudo I. and Kondo T., Chem. Engng Sci. 1978 33 315.
- [2] Sada E., Kumazawa H., Kudo I. and Kondo T. under contribution.

(Received January 16, 1980)